

COMPARISON BETWEEN THEORETICAL FORMULA AND EXPERIMENTAL RESULTS ON BUBBLE ELECTROPHORESIS^①

Xu Jirun[†], Kelsall G H[†]

[†] P. O. Box 139, Northeastern University, Shenyang 110006

[†] Imperial College of Science and Technology, London, England

ABSTRACT In the previous work, Xu Jirun and Kelsall G H have derived a new formula for bubble electrophoretic mobility by taking the internal circulation, surface charge perturbation and interface tension gradient into account. A comparison of the theoretical formula with the experimental results was given and some new aspects of the bubble electrophoresis were discussed in the present paper. It was shown that the new formula can predict the experimental facts, such as the dependence of electrophoretic mobility on bubble size and on electrical field direction that can not be explained by classical electrophoretic theory.

Key words bubble electrophoresis electrophoretic mobility bubble size electrical field

1 INTRODUCTION

Since 1861 Quincke^[1] first studied the electrophoretic phenomenon of bubbles, a lot experimental observations have been made (Brandon^[2] and Yurdakul^[3] made good reviews on this subject, respectively). However the theoretical prediction of the bubble electrophoresis is still far from satisfaction.

Booth^[4] is the first person who made systematically theoretical analysis of the electrokinetic phenomena of non rigid particles, including liquid drops and gas bubbles. He derived the electrophoretic mobility of fluid spheres, U_E , as follows:

$$U_E = \frac{\epsilon \xi}{6\pi\eta} \times [3\eta'(1 + \lambda) + 2\eta(1 - 2\lambda)] / (3\eta' + 2\eta) \quad (1)$$

where η' , η — the fluid viscosity within and outside the drop or bubble respectively; ϵ — the relative dielectric constant of the solution; ξ — the potential on the shear plane; $\lambda = (K - K') / (2K + K')$, and where K' and K represent the conductivity of the fluids inside and outside

the particle. Unfortunately, the application of Booth's formula to bubbles leads to the conclusion that bubbles have zero electrophoretic mobility (because $\eta' = 0$, $K' = 0$ and $\lambda = 1/2$ for bubbles), which is contradictory to the observed facts. Sengupta^[5] introduced surface conductivity to modify Booth's theory and obtained the bubble electrophoretic mobility as

$$U_E = \frac{\epsilon \xi}{2\pi\eta} \times \frac{K_s}{K_s + Ka} \quad (2)$$

where K_s is the specific surface conductivity and a is the bubble diameter. The formula shows that the bubble electrophoretic mobility is inversely proportional to the bubble size, which, however, is inconsistent with the experimental observations^[2, 3]. Jordan and Taylor^[6] gave their formula by considering the influence of the internal circulation in bubbles on the Stokes friction:

$$U_E = \frac{3\eta' + 3\eta}{3\eta' + 2\eta} \times \frac{\epsilon \xi}{6\pi\eta} \times [1 + \kappa(Ka)] \quad (3)$$

where κ is the Debye-Huckel parameter. The formula has no essential difference with the

classical theory and does not agree with the observed facts.

In their research on the charged mercury drop, Frumkin and Levich^[7] derived a formula:

$$U_E = \frac{a\sigma}{3\eta + 2\eta + \delta^2/\lambda} \quad (4)$$

where σ is the charge density on the shear plane. Having analysed the big difference between Eqn. (1) and Eqn(4), as both are used for mercury drops, Levince and O' Brien^[8] presented another electrophoretic mobility expression for mercury drops:

$$U_E = \frac{a\sigma}{3\eta + 2\eta} \times \left[1 - \frac{\sigma^2}{\lambda(3\eta + 2\eta)} \right] \quad (5)$$

Eqns. 4 and 5 predict a linear relationship between electrophoretic mobility and drop size. However they cannot be used for bubbles since mercury drops are assumed to be ideally polarizable^[3].

In our previous work, we have derived a new formula for bubble electrophoretic mobility^[9]. In the present paper, we only give the formula and our aim is mainly at the comparison of the theoretical formula with experimental results obtained by other authors. The formula derived by authors is expressed as

$$U_E = - \frac{2\sigma^0(\eta + 2\eta)}{3\eta(2\eta + 3\eta)} \times \left[\frac{\delta\Psi_{am}^E}{E} - a(1 + \lambda) \right] \quad (6)$$

where $\delta\Psi_{am}^E$ is the maximum surface potential perturbation due to the surface charge redistribution caused by the electrical field, E ; σ^0 is the equilibrium surface charge density, and related to the equilibrium surface potential Ψ_a^0 :

$$\begin{aligned} \sigma^0 &= - \frac{\epsilon_r}{4\pi} \left(\frac{d\phi^0}{dr} \right)_{r=a} \\ &= - \frac{\pm \epsilon_r}{4\pi} \left\{ \frac{8\pi kT}{\epsilon_r} \left[\sum n_{i0} \times \right. \right. \\ &\quad \left. \left. \exp\left(-\frac{Z_i e \Psi_a^0}{kT}\right) - \sum n_{i0} \right] \right\}^{1/2} \end{aligned} \quad (7)$$

where n_{i0} is the numerical concentration of i ion in bulk solution; Z_i is the valence of the i ion; e is the electronic charge; k is the Boltzman constant and T is the absolute temperature. The

selective signs in Eqn. 7 are dependent on the surface potential Ψ_a^0 , the positive is chosen for $\Psi_a^0 < 0$ and negative for $\Psi_a^0 > 0$. If $U_E > 0$, the electrophoretic mobility is along the electrical field direction, otherwise against. The potential perturbation caused by the external electrical field, Ψ_{am}^E , has its own sign which is determined by the sign of surface equilibrium potential, Ψ_a^0 , and the direction of the applied electrical field E . The sign selection is summarised in Table 1.

Table 1 Sign selection

E	Ψ_a^0	$\delta\Psi_{am}^E$	$\delta\Psi_{am}^E / E$	\pm Sign in Eqn. 7
– (Downward)	–	–	+	+
– (Upward)	–	+	+	+
– (Downward)	+	–	+	–
– (Upward)	+	+	+	–

2 EXPERIMENTAL ARRANGEMENTS AND RESULTS

There are three basic arrangements of the external electrical field and bubbles developed for measuring the bubble electrophoretic mobility. The first one is shown in Fig. 1(a) where a spinning cell is closed at ends by disk electrodes, bubbles are centrifuged to the axis, and the horizontal velocity under the applied electrical field is measured. This method was designed in the earlier researches^[1, 10–12] and is still used recently^[13]. Fig. 1(b) is the second widely used design^[2, 14–16] in which the electrical field is applied horizontally and the tested bubble has two velocity components: the rise velocity due to the buoyancy and the horizontal velocity (electrophoretic mobility) due to the electrical field. The third method, illustrated in Fig. 6(c), was developed by Yurdakul and Kelsall^[3] recently to measure the bubble rise velocity variation (electrophoretic mobility) with and without the electrical field. The characteristics of the design is the external electrical field is arranged to be parallel to the bubble rise direction. The influence of the different electrical arrangements on the bubble behaviour will be briefly discussed later.

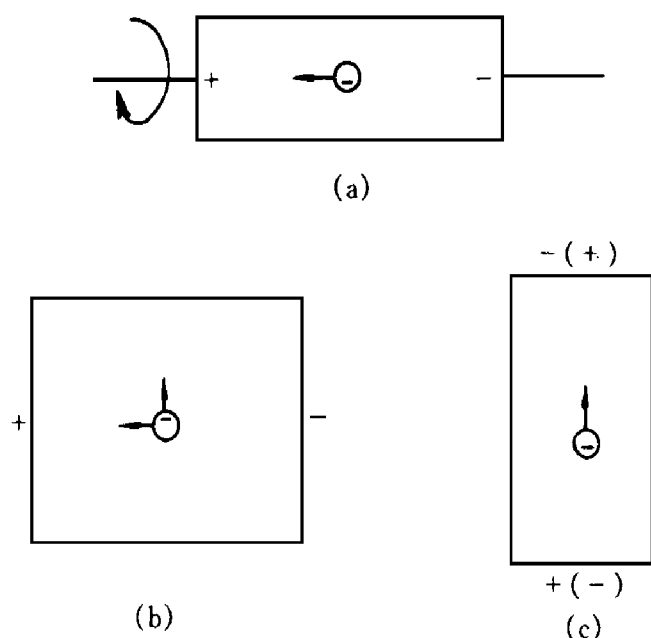


Fig. 1 Arrangements of external electrical field and bubbles

Brandon *et al*^[2] examined the bubble electrophoretic mobility in the absence of surfactants under a horizontally applied electrical field. Their typical results are given in Fig. 2 and Fig. 3. Yurdakul^[3] measured the bubble electrophoretic mobility in the absence of surfactants under a vertically applied electrical field with Laser Doppler Anemometer. He found the dependence of bubble electrophoretic mobility on the external electrical field direction (See Fig. 4)

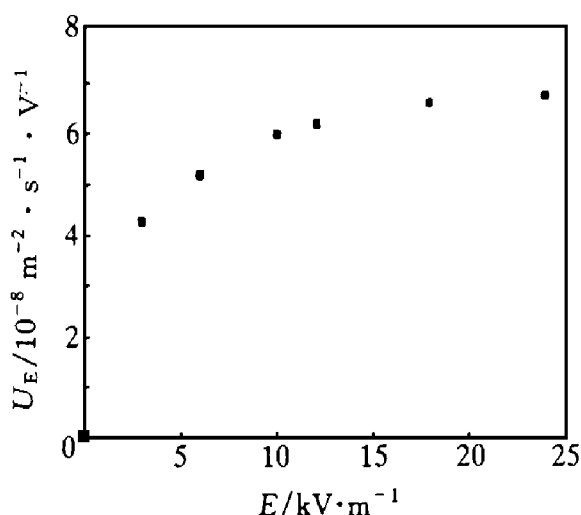


Fig. 2 Influence of bubble diameter on the electrophoretic mobility

(electrical field arranged as Fig. 1(b))^[2]

○—pH= 10; ○—pH= 8; ●—pH= 6; ○—pH= 4

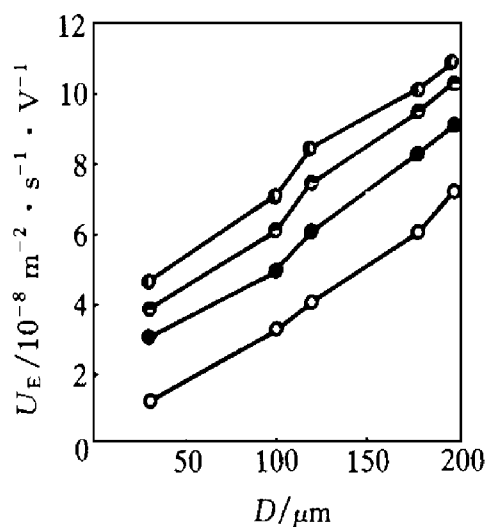


Fig. 3 Influence of electrical field strength on the electrophoretic mobility (horizontally applied electrical field, pH= 6.8, $a = 50 \mu\text{m}$)^[2]

besides something similar to Fig. 3. Obviously, these experiments show something that can not be explained by the classical electrophoretic theories.

3 COMPARISON AND DISCUSSION

Analysing Figs. 2, 3, 4 and Eqn. 6, it can be found that the theoretical prediction is in good agreement with the experimental results. The following are a few aspects which help us to reach the conclusion.

(1) The theoretical formula shows that there is a linear relationship between the electrophoretic mobility and bubble size, which is wonderfully verified by the experiments (Fig. 2). According to the theoretical analysis and the experimental facts, probably it is reasonable to conclude that the bubble electrophoretic mobility is directly proportional to the bubble size as long as there exists internal circulation within the bubble. This may be expanded to liquid drops in theory although we have not yet found the correspond experimental reports.

(2) The theoretical formula (Eqn. 6) predicts a dependence of the bubble electrophoretic mobility on the electrical field strength, which is also confirmed by experiments. Because $\delta\Psi_{\text{am}}^E/E$ is always greater than or equal to zero and re-

duces in value with the increase of the external field, the mobility, according to Eqn. 6, goes up at first with the field strength E and ultimately reaches an equilibrium value as E is big enough to make $\delta\Psi_{am}^E/E$ be zero, just as shown by experiments (See Figs. 3 and 4).

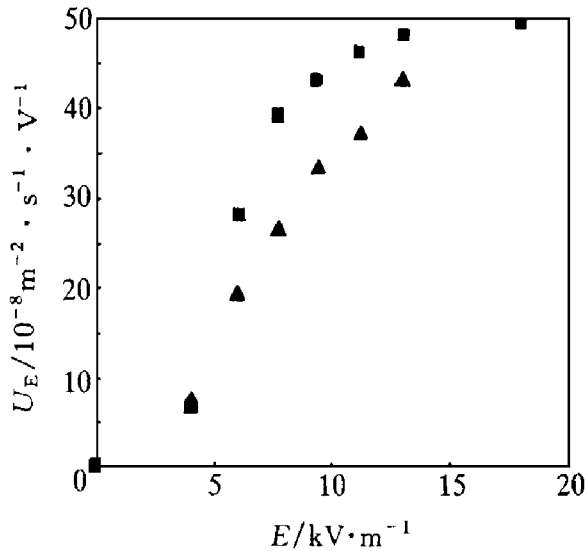


Fig. 4 Influence of electrical field strength and direction on the electrophoretic mobility (vertical applied electrical field, pH= 7.9, $a = 35 \mu\text{m}$)^[3]
 ▲ —downward field; ■ —upward field

(3) The influence of the electrical field direction on the electrophoretic mobility (Fig. 4) can also be explained satisfactorily by the theoretical formula. Experimental results illustrate that for vertically applied electrical field and negatively charged bubbles, the electrophoretic mobility under upward electrical field has higher values than that under downward field, and if the field strength is big enough, the difference tends to disappear. Let us see how the theoretical formula, Eqn. 6, predict the fact above. For a negatively charged bubble, the electrophoretic mobilities under upward and downward electrical field are expressed by Eqns. 8 and 9 respectively (Refer to Eqn. 6 and Table 1):

$$U_{E+} = - \frac{2\sigma^0(\eta + 2\eta')}{3\eta(2\eta + 3\eta')} \times \left[\frac{\delta\Psi_{am}^{E+}}{E} - a(1 + \lambda) \right] \quad (8)$$

$$U_{E-} = - \frac{2\sigma^0(\eta + 2\eta')}{3\eta(2\eta + 3\eta')} \times \left[\frac{\delta\Psi_{am}^{E-}}{E} - a(1 + \lambda) \right] \quad (9)$$

It can be seen that if

$$|\delta\Psi_{am}^{E+}| = |\delta\Psi_{am}^{E-}|$$

the mobility value should be independent on the field direction; however, because of the uneven charge distribution on the bubble surface before the external field applied, the charge movement downward along the surface has to overcome more electrical resistance between surface charges than the charge movement upward does, which leads to $|\delta\Psi_{am}^{E+}| < |\delta\Psi_{am}^{E-}|$, $|u_{E+}| > |u_{E-}|$ at the same field strength. Similarly, if the bubble is charged positively, it is easy to come to an opposite conclusion: $|u_{E+}| < |u_{E-}|$. If the external electrical field E , either upward or downward, is rather large, the values of $\delta\Psi_{am}^E/E$ tend to zero, then the influence of the field direction is so small that it can not be observed experimentally. As for the horizontally applied electrical field, it is obvious that the electrical field direction does not affect the surface charge distribution pattern, therefore the experiments (Fig. 3) did not find the phenomenon shown in Fig. 4.

(4) Experimental results indicated that the bubble electrophoretic mobility increases with pH (See Fig. 2), which is also predictable from the theoretical formula if we take into account the mechanism in which the bubble is charged. According to Brandon^[2], the surface charge of a bubble comes from the competitive adsorption of the cations and anions in the solution, while the anions tend to be less hydrated and more polarised and therefore are specially adsorbed. This is the reason why bubbles are usually negatively charged. With the increase of pH value, there are more $[\text{OH}]^-$ adsorbed on the bubble surface, then the surface charge density σ^0 enlarges and the electrophoretic mobility speeds (See Eqn. 2).

Substituting the electrophoretic mobility values obtained experimentally into the theoretical formula Eqn. 6 or 7, the surface equilibrium potential, Ψ_a^0 , the surface equilibrium charge

density, σ^0 , as well as the potential perturbation, $\delta\Psi_{am}^E$, can be estimated. Taking the experimental results in Fig. 4 as examples, by extrapolating the electrical field strength to 18 kV/m at which the two curves in Fig. 4 predict equal mobility (about $50 \times 10^{-8} \text{ m}^2 \cdot \text{s}^{-1} \cdot \text{V}^{-1}$) and the term $\delta\Psi_{am}^E/E$ is negligible, we get the values of Ψ_a^0 and σ^0 as follows:

$$\Psi_a^0 = -1.11 \text{ mV},$$

$$\sigma^0 = -2.53 \times 10^{-5} \text{ C/m}^2$$

which are much smaller than that predicted by Smoluchowski equation. This is not difficult to understand, because the Smoluchowski equation is valid for the situation where no circulation takes place within the bubble, or in other words, all the bubble surface is occupied by the adsorbed charges. Therefore, it is clear that the classical electrophoretic theory not only can not explain the experimental phenomena but also overestimates the surface charge or potential too much as there exists internal flow inside bubbles.

The calculated $\delta\Psi_{am}^E$ vs electrical field E is drawn in Fig. 5. It is seen that the potential perturbation generated by the applied electrical field reaches its maximum at a certain field strength and then reduces its value with the increase of the field. Noting that the resistance to charge movement on the surface should very be similarly with the field strength, the result above is understandable.

In the end of this section, we are interested in making some comments on the different arrangements of the electrical field and bubbles shown in Fig. 1 by examining the surface charge distribution. The surface charge distribution patterns for the three cases in Fig. 1 are illustrated in Fig. 6. It is clear that as the external electrical field is exerted vertically (Fig. 1(c)), the charge distribution on the bubble surface is always axis-symmetric about the field direction (Fig. 6(c)); if the field applied horizontally and the rise rate allowed (Fig. 1(b)), the surface charges tend to concentrate on one side of the bubble bottom then the distribution pattern is asymmetric about the electrical field (Fig. 6(b)); as for the case of Fig. 1(a), although the charge distribution (Fig.

6(a)) is similar to Fig. 6(c), the spinning cell, according to Huddleston and Smith^[18], decreases the sensitivity of the electrophoretic measure. Thereafter, in general, the vertically applied electrical field is more suitable than other two arrangements.

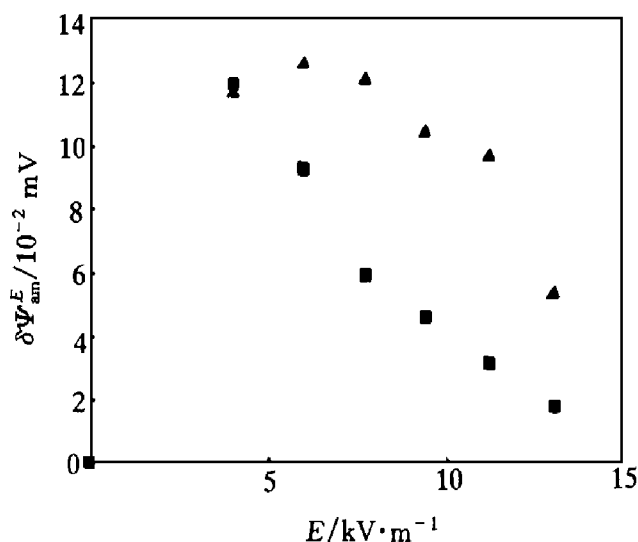


Fig. 5 Calculated relation of $\delta\Psi_{am}^E$ vs E
 ▲—downward field; ■—upward field

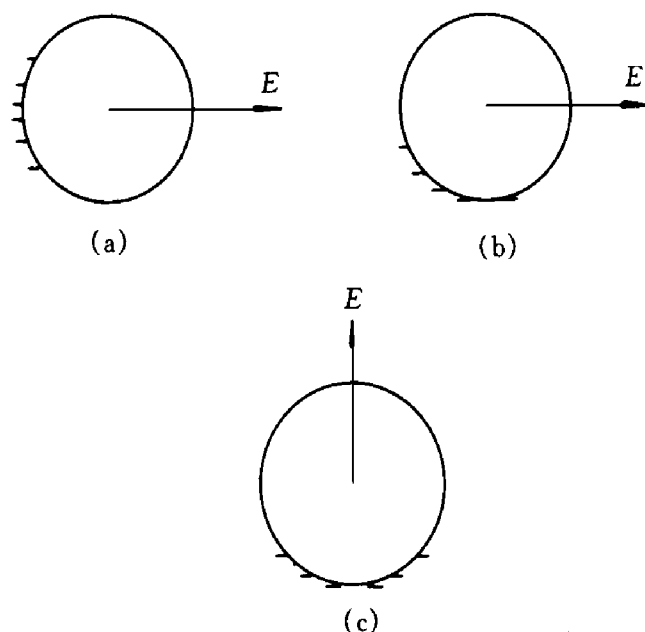


Fig. 6 Surface charge distribution patterns and field direction

- (a) —with spinning and horizontal velocity;
 (b) —with vertical and horizontal velocity;
 (c) —with only vertical velocity

(To page 129)

regarded as free electronic gas, so we can describe the thermal conductivity of free electrons by using thermal conductivity formula of ideal gas^[5]:

$$K_e = 1/3 C_v^e \cdot V \cdot L$$

where C_v^e is electron thermal capacitance per unit volume; V is average speed of free electrons; L is mean free path. As far as alloy is concerned, the existence of solute elements will diminish the mean free path of free electron and then cut down the average speed, so we can learn from formula(3) that thermal conductivity of alloy is less than that of pure metal. This difference will be obvious in the case of cryogenic temperature at which the thermal conductivity is mainly caused by free electrons.

4 CONCLUSIONS

(1) Thermal conductivity of pure Al and Al-Li alloy changes with temperature. Thermal conductivity of experimental sample first increases with temperature from low degree(4K) to the

maximum at (30~50 K) and then decreases with increasing temperature.

(2) Temperature with maximum value of K keeps stable roughly with increasing Li content, but the value of K decreases.

(3) Thermal conductivity of Al and Al-Li alloy is mainly caused by electron thermal conductivity and also affected by solute atoms and lattice defects.

REFERENCES

- 1 Sun Dongsheng, Li Fengzhao, Zhang Gang. *Acta Metall Sinica*, 1992, 6A(2): 78-88.
- 2 Glazer J, Verzasconis L, Sawtell R R. *Metall Trans*, 1987, 18A: 1695.
- 3 Chen E. In: *Proc of 6th Inter Al-Li Conf*, 1991: 445.
- 4 Huang Kun, Han Ruqi. *Solid State Physics*, (in Chinese). Beijing: Higher Education Press, 1988: 150.
- 5 Wang Run. *Physical Characteristic of Metal Materials*, (in Chinese). Beijing: Metallurgical Industry Press, 1985: 161.

(Edited by Li Kedi)

(From page 10)

4 SUMMARY

The internal circulation within bubbles results in a series of special electrophoretic phenomena, such as the dependence of electrophoretic mobility on the bubble size and the electrical field direction. These can not be explained by the classical electrophoresis theories. In the previous work, authors have advanced a new formula to describe the bubble electrophoretic mobility. The aim of this paper is at the verification of the formula experimentally. We are satisfactory to point out that the experimental results are all predictable according to the new-derived theoretical formula(Eqn. 6).

REFERENCES

- 1 Quincke G. *Ann Pogg*, 1961, 113: 513.
- 2 Brandon N P. PhD thesis. Imperial College, 1985.
- 3 Yurdakul S. PhD thesis, Imperial College, 1991.

- 4 Booth F. *J Chem Phys*, 1951, 19: 1331.
- 5 Sengupta M. *Indian J Chem*, 1968, 6: 501-505.
- 6 Jordan D O, Taylor A. *J Trans Faraday Soc*, 1952, 48: 346.
- 7 Frumkin A N, Levich V G. *Acta Physicochim*, 1946, 21: 193.
- 8 Levine S, O'Brien R N. *J of Coll and interface Sci*, 1973, 43(3): 616-629.
- 9 Xu Jirun, Kelsall G H. *Trans Nonferrous Met Soc China*, 1996, 6(3): 10.
- 10 Alty T. *Proc Roy Soc*, 1924, A106: 315.
- 11 McTaggart H A. *Phil Mag*, 1922, 44: 386.
- 12 Buch N, Gilman A. *Acta Physicochim*, 1938, 9, 1.
- 13 Sakai M. *Progr Colloid & Polymer Sci*, 1988, 77: 136.
- 14 Collins G L, Motarjemi M, Jameson G J. *J Coll Interface Sci*, 1978, 73: 69.
- 15 Fukui Y, Yuu S. *A I Ch E J*, 1982, 28: 866.
- 16 Kubota K, Hayashi S, Inaoka M. *J Coll Interface Sci*, 1983, 95: 362.
- 17 Brandon N P, Kelsall G H, Levine S *et al.* *J Appl Electrochem*, 1985, 475: 15.
- 18 Huddleston R W, Smith A L. "Foams" In: Aker R J ed. London: Academic Press, 1976: 147.

(Edited by Wu Jiaquan)